Journal of Mathematical Chemistry Vol. 34, Nos. 1–2, July 2003 (© 2003)

Simulation of non-linear flow density in transition state from the mathematical model of the diffusion of metal anions through a flat sheet supported liquid membrane

G. Benzal [a], A. Kumar [b], A.M. Sastre [c] and A. Delshams [d]

[a] *Department of Mathematics of the School of Chemistry Universidad Nacional de Tucumán, Tucumán, Argentina, Ayacucho 490, 4000*
[b] *PREFRE, Bhabha Atomic Research Centre, Tarapur, India*
[c] *Department of Chemical Engineering, Universitat Politècnica de Catalunya, ETSEIB, Barcelona, Diagonal 647, E-08028, Spain*
[d] *Department of Applied Mathematics I, Universitat Politècnica de Catalunya, ETSEIB, Barcelona, Diagonal 647, E-08028, Spain*

Received 16 September 2002

A mathematical model is developed for the carrier facilitated transport of metal ions through a flat sheet support liquid membrane (FSSLM) in transition state from Fick's second law. From this model, and from Fick's first law, the flow density is derived as a non-linear concentration gradient. Both expressions, concentration and flow density, depend on the thickness of the membrane and on time. Since the rate constant plays an important role in the model, it is considered as the parameter that controls the system and an equation for it is obtained. This equation explains the velocity of the co-transport process. The proposed model takes into account the species co-transported together with the metal ions. An equation for the number of moles of this species is obtained as a function of the metal species. The concentration gradient of this species explains the behaviour of pH in the feed phase during the process. The model is tested against experimental data corresponding to the transport of metal anions in acidic solution and it is shown that the co-transport process is reproduced with high accuracy.

1. Introduction

The transport of molecules and ions across liquid membranes represents a powerful new tool that excels most conventional separation techniques since it combines extraction, scrubbing and regeneration into a single step.

The separation and concentration of materials is a very important operation and has a long history of improvement and diversity.

Membranes for separation and concentration possess such characteristics as expediency of operation, energy related advantages, lack of side reactions and high functional capacity, and they have environmental applications in a wide variety of fields such as hydrometallurgy, biotechnology and the nuclear field.

0259-9791/03/0700-0001/0

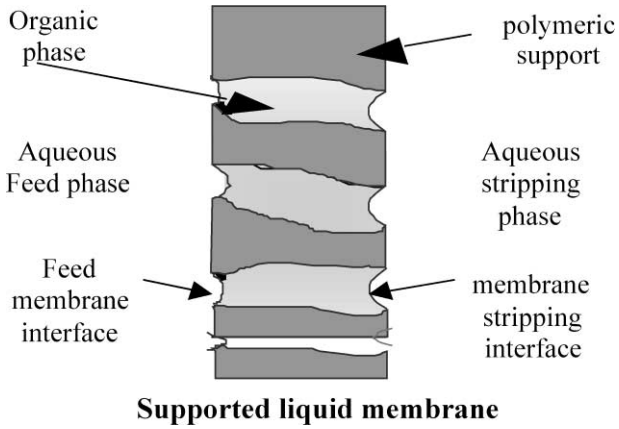

Figure 1. Schematic representation of the flat sheet supported liquid membrane.

Liquid membranes are expected to play a leading role in science and technology in the near future, and continuous efforts are being made to develop improved functions in these membranes [1,2].

A general modelling is proposed in this work from the analysis of the co-transport of metal ions through a flat sheet supported liquid membrane. To understand the modelling a description of the system is introduced (further details of this process are described elsewhere [3–7]).

The FSSLM system is represented in figure 1 and the co-transport mechanism is described schematically in figure 2. From figure 1, the FSSLM is assumed to be composed of the following three phases and two interfaces:

- *Aqueous feed phase*. Initially, the total metal anions are contained in this phase.
- *Feed-membrane interface*. In this interface a chemical reaction takes place to form the metal complex.
- *Membrane phase*. This is a polymeric support impregnated with an organic solvent containing an extractant (carrier) and a diluent. The metal complex diffuses through the organic phase up to the stripping interface.
- *Membrane-striping interfaces*. In this interface another chemical reaction takes place.
- *Aqueous stripping phase*. Initially, this phase is free of metal and contains a stripping agent in order to facilitate the decomplexation of the metal complex to the stripping phase.

It is important to note that the development of the theoretical model that simulates the co-transport across the FSSLM is fundamental for a complete understanding of transport mechanisms and also to predict the value of non-measurable parameters. Therefore, the objective of this paper is to perform a mathematical modelling of facilitated co-transport in transition state and from this model to derive the

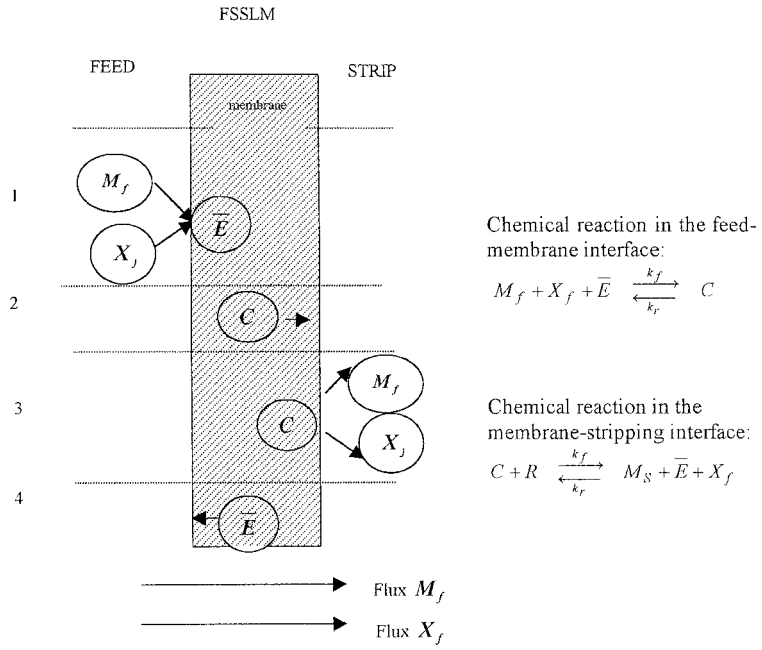

Figure 2. Schematic representation of the co-transport mechanism across the FSSLM.

flow density inside the membrane in terms of the time and the thickness of the membrane.

2. Modelling

The modelling of FSSLM system is divided into three different but interrelated parts: the feed phase, the membrane phase and the stripping phase, taking into account the phenomena that take place in each of them, and relating these phases by means of the feed-membrane interface and the membrane-stripping interface. In the FSSLM system, apparent rate constants of the chemical reaction play an important role [8–10]. These constants are considered as kinetic parameters, as explained below.

In addition, some assumptions are needed to model and analyse the results obtained. In the present model, the assumptions taken into account are:

- The non-stirred layer is reduced to the Nernst film. Therefore, the diffusion in the feed phase is not considered.
- The extractant concentration is constant throughout the process.
- The equilibrium constant is calculated experimentally.
- The pressure and temperature are constant.
- The driving force of the FSSLM system is defined as the gradient concentra-

tion between the aqueous phases (feed phase and stripping phase) of the species which are co-transported with the metal.

- The reactions in both, the feed-membrane and membrane-stripping interfaces are very fast and complete.

Taking into account the assumptions and the mechanism of the co-transport process, the modelling is discussed in each phase for clarity.

2.1. Aqueous feed phase

As can be seen in figure 2, the chemical reaction that takes place at the feed-membrane interface can be written as

$$M_{\mathrm{f}} + X_{\mathrm{f}} + \overline{E} \underset{k_{\mathrm{r}}}{\overset{k_{\mathrm{f}}}{\rightleftarrows}} \overline{C}. \tag{1}$$

The chemical reaction (1) is modelled by kinetics equations. In this type of facilitated transport, metal ions, M_{f}, can be transported across the membrane against their concentration gradient. The transport occurs at the expense of a large chemical potential gradient existing between the two opposite sides of the membrane.

The difference of concentration of the species X_{f} between the feed and the stripping phase gives rise to the gradient concentration, which is considered as the driving force of the process. This species X_{f} plays an important role in the co-transport as shown in figure 2.

Therefore, the first step will be to obtain a mathematical equation that describes the concentration of the species X_{f} denoted by $[X_{\mathrm{f}}]$ in terms of the metal concentration of the species M_{f}, denoted by $[M_{\mathrm{f}}]$. The two are modelled simultaneously. A detailed description of the modelling in the feed phase and its corresponding solutions are derived in this section.

From the reaction (1), the kinetics equations and the initial conditions in terms of the number of moles are:

$$\begin{aligned}
&\frac{\mathrm{d}n_{\mathrm{f}}}{\mathrm{d}t} = -k_1 n_{\mathrm{f}} n_{X_{\mathrm{f}}} n_{\overline{E}} + k_2 n_{\overline{C}},\\
&\frac{\mathrm{d}n_{\overline{C}}}{\mathrm{d}t} = k_1 n_{\mathrm{f}} n_{X_{\mathrm{f}}} n_{\overline{E}} - k_2 n_{\overline{C}},\\
&n_{\mathrm{f}}(0) = n_0; \quad n_{\overline{C}}(0) = 0 \quad \text{(initial conditions)}.
\end{aligned} \tag{2}$$

The apparent rate constants deduced from (2) can be expressed as

$$k_1 = \frac{k_{\mathrm{f}}}{A_{\mathrm{eff}}^2}, \tag{3}$$

$$k_2 = k_{\mathrm{r}}. \tag{4}$$

It is worth noting that these constants depend on the effective interfacial area A_{eff}, which is the geometric area of the membrane times the porosity, ε, of the membrane.

Table 1
Several cases where the mathematical model can be applied. The relation $[Y]$ represents the concentration of cations and/or anions. The charge of ions are represented by n and m.

Case 1	*Case* 2	*Case* 3	*Case* 4
$C^{n+}ML^{n-} + B(OH)_m$,	$C^{n-}ML^{n+} + H_mA$,	$C^{n+}ML^{n-} + H_mA$,	$C^{n-}ML^{n+} + B(OH)_m$
$M_f = ML^{n-}$	$M_f = \begin{cases} ML^{n+} \\ M^{n+} \end{cases}$	$M_f = ML^{n-}$	$M_f = \begin{cases} ML^{n+} \\ M^{n+} \end{cases}$
		Case 3(a)	*Case* 4(a)
		$X_f = [H^+]$,	$X_f = [OH^-]$,
		$[H^+] = [Y] + q[M_f]$,	$[OH^-] = [Y] + q[M_f]$,
		$[Y] = m[A^{m-}]$	$[Y] = m[B^{m+}]$
		$-n[C^{n+}]$,	$-n[C^{n-}]$,
		$q = n$	$q = n$
Case 1(b)	*Case* 2(b)	*Case* 3(b)	*Case* 6(b)
$X_f = [C^{n+}]$,	$X_f = [C^{n-}]$,	$X_f = [C^{n+}]$,	$X_f = [C^{n-}]$,
$[C^{n+}] = [Y] + q[M_f]$,	$[C^{n-}] = [Y] + q[M_f]$,	$[C^{n+}] = [Y] + q[M_f]$,	$[C^{n-}] = [Y] + q[M_f]$,
$[Y] = \frac{1}{n}[OH^-]$	$[Y] = \frac{1}{n}[H^+]$	$[Y] = \frac{1}{n}[A^{m-}]$	$[Y] = \frac{1}{n}[B^{m+}]$
$-\frac{m}{n}[B^{m+}]$,	$-\frac{m}{n}[C^{n-}]$,	$-\frac{m}{n}[H^+]$,	$-\frac{m}{n}[OH^-]$,
$q = 1$	$q = 1$	$q = 1$	$q = 1$
Case 1(c)	*Case* 2(c)		
$X_f = [B^{m+}]$,	$X_f = [A^{m-}]$,		
$[B^{m+}] = [Y] + q[M_f]$,	$[A^{m-}] = [Y] + q[M_f]$,		
$[Y] = \frac{1}{m}[OH^-]$	$[Y] = \frac{1}{m}[H^+]$		
$-\frac{n}{m}[C^{n+}]$,	$-\frac{n}{m}[C^{n-}]$,		
$q = \frac{n}{m}$	$q = \frac{n}{m}$		

It is necessary to take A_{eff} into account, because the chemical reaction (1) takes place in a heterogeneous medium (between two different phases) [11,12].

The distribution of a solute between two different phases is modified by the presence of various species and in some cases the extraction is favoured. A particular case is the association with the protons and the influence of the pH in the extraction technique, because when the medium is acidic the transport is facilitated in contrast to what happens when the medium is basic. In cases where the medium is basic, the solutions of the modelling are different. This modelling is discussed in [13].

The mechanism of co-transport modelled in this paper is described in figure 2 and is valid for all the cases presented in table 1.

To complete the kinetics equations of the chemical reaction (1), it is necessary to obtain a model of the species X_f responsible for the co-transport.

In order to model the concentration of the species X_f, the electro-neutrality principle corresponding to the feed phase is taken into account. Starting from this principle and the analysis of the aqueous solution present in the feed phase, acidic or basic, several possibilities are analysed and introduced in table 1. From this table, the equation for the concentration of the species X_f is given by

$$\left[X_f(t)\right] = [Y] + q[M_f](t), \tag{5}$$

where $[M_\mathrm{f}] = n_\mathrm{f}/V_\mathrm{wf}$ is the concentration of the metal species and $[X_\mathrm{f}] = n_{X_\mathrm{f}}/V_\mathrm{wf}$ is the concentration of the species X_f, both at any time in the feed phase.

The references for $[Y]$ and q are explained in table 1. The notation $[\cdot]$ indicates the concentration in the aqueous phase. The notation $[\overline{\cdot}]$ refers to concentrations in the membrane phase.

Therefore, the number of moles of the species X_f is expressed as

$$n_{X_\mathrm{f}}(t) = n_Y + q n_\mathrm{f}(t). \tag{6}$$

It is worth to note that in the cases $\mathrm{C}^{n+}\mathrm{ML}^{n-} + \mathrm{B(OH)}_m$ and $\mathrm{C}^{n-}\mathrm{ML}^{n+} + \mathrm{H}_m\mathrm{A}$ (see cases 1(b) and 2(b) in table 1), the species X_f follows a different relation with respect to the metal species, which is considered in [13].

Introducing the equation (6) in the kinetics equations (2) the following dynamical system for the number of moles of the metal in the feed phase is obtained:

$$\begin{aligned}
&\frac{\mathrm{d}n_\mathrm{f}}{\mathrm{d}t} = -k_1 n_\mathrm{f} n_{X_\mathrm{f}} n_{\overline{E}} + k_2 n_{\overline{C}},\\
&\frac{\mathrm{d}n_C}{\mathrm{d}t} = k_1 n_\mathrm{f} n_{X_\mathrm{f}} n_{\overline{E}} - k_2 n_{\overline{C}},\\
&n_{X_\mathrm{f}}(t) = n_Y + q n_\mathrm{f}(t),\\
&n_\mathrm{f}(0) = n_0; \quad n_C(0) = 0.
\end{aligned} \tag{7}$$

Instead of proceeding to the analytical resolution for system (7), first a mathematical stability analysis will be carried out [14,15], to provide us with the controlling parameter k_2 of the FSSLM system, together with an approximate expression for the solution of the dynamical system (7).

First, we note that (7) satisfies the identity $n_\mathrm{f} + n_C = n_0$ and this allows us to reduce it to the one-dimensional reduced system:

$$\begin{aligned}
&\frac{\mathrm{d}n_\mathrm{f}}{\mathrm{d}t} = F(n_\mathrm{f}) = -k_1 n_{\overline{E}} n_\mathrm{f}(n_Y + q n_\mathrm{f}) + k_2(n_0 - n_\mathrm{f}),\\
&n_\mathrm{f}(0) = n_0.
\end{aligned} \tag{8}$$

From the equation

$$F(n_\mathrm{f}) = 0 \tag{9}$$

two roots are obtained, but only one is admissible as the equilibrium point of the system and is denoted by n^f_∞. This value n^f_∞ represents the number of the moles of the metal in the feed phase when the steady state is achieved and therefore $M_\infty = n^\mathrm{f}_\infty/V_\mathrm{wf}$ is the corresponding metal concentration.

We recall that

- $n_0 = V_\mathrm{wf} M_0$ and $n_\mathrm{f} = V_\mathrm{wf}[M_\mathrm{f}]$ are the numbers of moles of the metal species in the aqueous volume V_wf of the feed phase (initially and at any time, respectively);

- $n_{\overline{E}} = V_0[\overline{E}]$ is the number of moles of the extractant species in the organic volume V_0 and $n_Y = V_{\mathrm{wf}}[Y]$ is the number of moles of the species $[Y]$ in the aqueous volume V_{wf}. Then, with this notation the value of M_∞ is computed as

$$M_\infty = \frac{-(K_{\mathrm{ex}}[\overline{E}][Y]+1) + \sqrt{(K_{\mathrm{ex}}[\overline{E}][Y]+1)^2 + 4M_0K_{\mathrm{ex}}q[\overline{E}]}}{2qK_{\mathrm{ex}}[\overline{E}]}. \tag{10}$$

  Moreover, the characteristic exponent λ is given by

$$\lambda = -\big(k_2 + K_{\mathrm{ex}}k_2[\overline{E}]\big([Y]+2qM_\infty\big)\big) < 0 \quad \forall k_2, \tag{11}$$

  where the equilibrium constant $K_{\mathrm{ex}} = k_1/k_2$ is related to both apparent rate constants k_1 and k_2 defined in (3) and (4).

The characteristic exponent λ given in (11) depends also on the initial conditions of the FSSLM system. It turns out that it is always negative, and as a consequence the equilibrium point M_∞ (or n_∞) is stable.

The value of λ (11) allows us to estimate the value of the apparent rate constant k_2, which will be considered the "controlling parameter of the model".

An important consequence is that the value of M_∞, jointly with the initial metal concentration M_0, predicts the metal extraction percentage $M_{\%E}$ through the rate:

$$M_{\%E} = \frac{M_0 - M_\infty}{M_0} \cdot 100.$$

We can now give an approximate expression to the analytical solution of dynamical system (7) in terms of the time, the equilibrium point, the controlling parameter and the initial condition of the system:

$$n_{\mathrm{f}}(t) = n_\infty^{\mathrm{f}} + \big(n_0 - n_\infty^{\mathrm{f}}\big)\exp(\lambda t), \quad t \geqslant 0. \tag{12}$$

From (12) one immediately gets an approximate expression for the metal concentration in the feed phase:

$$[M_{\mathrm{f}}](t) = \frac{n_{\mathrm{f}}}{V_{\mathrm{wf}}} = M_\infty + (M_0 - M_\infty)\exp(\lambda t), \quad t \geqslant 0. \tag{13}$$

In order to continue the modelling, equation (13) will be used to relate the two phases, feed and membrane phase (see figures 1 and 2).

2.2. Membrane phase

The membrane phase is where the diffusion of the metal-complex across the membrane takes place [16]. Fick's second law [17,18] describes the change of the concentration in transition states. Therefore, in this section, the concentration of metal-complex through the membrane is modelled by this law.

The total density, temperature and pressure are assumed to be constant, as is the diffusion coefficient of the solution, because only dilute solutions are considered. Due

to the system configuration, only one-dimensional diffusion across the membrane phase is kept in mind.

Throughout this section the following notation will be used. The function $u(x,t)$ represents the metal-complex concentration and depends on the time t and the thickness of the membrane, denoted by the spatial variable x. The behaviour of the metal-complex species through the membrane phase is modelled by the diffusion equation [16,17] (Fick's second law) with initial and boundary conditions as follows:

$$\frac{\partial u(x,t)}{\partial t} = D_{\text{eff}} \frac{\partial^2 u(x,t)}{\partial x^2}, \quad t > 0;\ 0 < x < L \tag{14}$$

(Fick's second law);

$$u(x,0) = 0, \quad 0 \leqslant x \leqslant L \tag{15}$$

(the initial condition (15) indicates that there is no metal complex in the membrane at the initial time, $t = 0$);

$$u(0,t) = \frac{V_{\text{wf}}}{V_0}\big(M_0 - [M_{\text{f}}]\big), \quad t > 0;\ \lambda < 0 \tag{16}$$

(free boundary conditions in the feed-membrane interface $x = 0$).

Since the system is heterogeneous (the chemical reaction takes place in interfaces), the source term $u(0,t)$ in the condition (16) is obtained from (13) and denotes the metal-complex generation. Therefore, it can be incorporated as a boundary condition (16) just on the surface (feed-membrane interface) where the chemical reaction (1) arises [15]. Condition

$$\frac{\partial u(L,t)}{\partial x} = 0 \quad \forall t > 0 \tag{17}$$

(insulated boundary condition in the membrane-stripping interface, $x = L$)

indicates that metal-complex does not flow to the stripping phase.

The solution of the model (14)–(17) is obtained by means of eigenfunction expansion methods [19,20] and is given by

$$u(x,t) = \frac{V_{\text{wf}}}{V_0}(M_0 - M_\infty)\big(1 - \exp(\lambda t)\big) + \frac{V_{\text{wf}}}{V_0}\sum_{i=1}^{\infty} b_i(t)\phi_i(x,\lambda_i), \tag{18}$$

where the temporal Fourier coefficients $b_i(t)$,

$$b_i(t) = \frac{4}{\pi}\lambda \frac{(M_0 - M_\infty)}{(2i-1)(\lambda + \lambda_i D_{\text{eff}})}\big(\exp(\lambda t) - \exp(-\lambda_i D_{\text{eff}} t)\big), \quad i = 1, 2, \ldots, \tag{19}$$

are obtained from Fourier analysis.

It is important to distinguish between the eigenvalue λ, obtained from the mathematical stability study introduced in (11) and the eigenvalues

$$\lambda_i = \frac{(2i-1)^2\pi^2}{4L^2}, \quad 0 \leqslant x \leqslant L,\ t \geqslant 0,\ i = 1, 2, \ldots$$

obtained by the method of separation of variable by Fourier series, where

$$\phi_i(x, \lambda_i) = \sin\sqrt{\lambda_i}x, \quad i = 1, 2, \ldots$$

are the corresponding eigenfunctions.

In (14), D_{eff} is the diffusion coefficient of the metal-complex defined as $D_{\text{eff}} = D_E\varepsilon/\tau^2$ [21]. This coefficient plays an important role in the diffusion process. It is related to the diffusion coefficient of the extractant in the organic phase, denoted by D_E and the porosity ε and the tortuosity τ of the support of the FSSLM. This is essentially the same as the diffusion coefficient of the metal-complex, because the size of the metal ion [5] is much smaller than the extractant molecule diffusion coefficient of the extractant in the organic phase.

The concentration of the metal-complex species in the first and second interfaces are obtained from the solution (18) respectively for $x = 0$ and $x = L$.

If $x = 0$, it is clear that

$$u(0, t) = \frac{V_{\text{wf}}}{V_0}(M_0 - M)\big(1 - \exp(\lambda t)\big)$$

represents the metal-complex concentration in the feed-membrane interface (first interface) and

$$n_{\text{m}}(0, t) = V_0 u(0, t) = \big(n_0 - n_\infty^{\text{f}}\big)\big(1 - \exp(\lambda t)\big) \tag{20}$$

is the corresponding number of moles. Equation (20) is in concordance with the boundary condition (16).

From (18), if $x = L$, one gets

$$u(L, t) = \frac{V_{\text{wf}}}{V_0}(M_0 - M_\infty)\big(1 - \exp(\lambda t)\big) + \frac{V_{\text{wf}}}{V_0}\sum_{i=1}^{\infty}(-1)^{i+1}b_i(t) \tag{21}$$

which represents the metal-complex concentration in the membrane-stripping interface (second interface) and therefore the corresponding number of moles is given by

$$n_{\text{m}}(L, t) = V_0 u(L, t) = \big(n_0 - n_\infty^{\text{f}}\big)\big(1 - \exp(\lambda t)\big) + V_{\text{wf}}\sum_{i=1}^{\infty}(-1)^{i+1}b_i(t). \tag{22}$$

The difference between the number of moles (20) and the number of moles (21),

$$\begin{aligned} N_{\text{m}}(t) &= n_{\text{m}}(0, t) - n_{\text{m}}(L, t) \\ &= \frac{4}{\pi}\lambda\sum_{n=1}^{\infty}(-1)^{i+1}\frac{(n_0 - n_\infty^{\text{f}})}{(2i-1)(\lambda + \lambda_i D_{\text{eff}})}\big(\exp(\lambda t) - \exp(-\lambda_i D_{\text{eff}} t)\big), \quad (23) \\ 0 \leqslant x < L,\ t \geqslant 0, \end{aligned}$$

is the number of moles inside the membrane without considering the second interface. The corresponding complex concentration is

$$\overline{U}(t) = \frac{N_{\mathrm{m}}(t)}{V_0} = -\frac{4}{\pi}\lambda\frac{1}{V_0}\sum_{n=1}^{\infty}(-1)^{i+1}\frac{(n_0 - n_{\infty}^{\mathrm{f}})}{(2i-1)(\lambda + \lambda_i D_{\mathrm{eff}})}\big(\exp(\lambda t) - \exp(-\lambda_i D_{\mathrm{eff}} t)\big). \tag{24}$$

Therefore, from (18) and (21) follows that the metal-complex concentration inside membrane (without the second interface) is represented by

$$u_{\mathrm{m}}(x,t) = u(x,t) - u(L,t). \tag{25}$$

As a final check, we note that the stability of the solution allows us to discover the behaviour of the metal-complex in the steady state. Indeed, it is easy to show that for any $0 \leqslant x < L$

$$\lim_{t\to\infty}\overline{U}(t) \to 0.$$

These results confirm the expected behaviour for the metal-complex in the steady state, that is, the metal ions will be recovered in the stripping phase.

2.2.1. Modelling and simulation of the flow density inside the membrane

The mathematical model of the facilitated co-transport developed above allows us to derive the flow density inside the membrane in terms of time t, and the membrane thickness x.

Indeed, differentiating (18) with respect to the thickness of the membrane and introducing it into Fick's first law $J = -D_{\mathrm{eff}}\partial u/\partial x$, the flow density $J(x,t)$ in transition state is given in terms of a "non-linear concentration gradient" as

$$\begin{aligned} J(x,t) &= -D_{\mathrm{eff}}\frac{\partial u(x,t)}{\partial x} \\ &= -D_{\mathrm{eff}}\frac{V_{\mathrm{wf}}}{V_0}\sum_{i=1}^{\infty} b_i(t)\frac{\partial}{\partial x}\sin\left(\frac{(2i-1)\pi x}{2L}\right) \\ &= -D_{\mathrm{eff}}\frac{\pi}{2L}\frac{V_{\mathrm{wf}}}{V_0}\sum_{i=1}^{\infty}(2i-1)b_i(t)\cos\left(\frac{(2i-1)\pi x}{2L}\right). \end{aligned} \tag{26}$$

Equation (26) allows us to simulate in a three-dimensional plot the behaviour of the flow density for any time and any membrane thickness. It is worth to note that the effective diffusion coefficient in the organic phase, D_{eff}, and the thickness of the membrane, denoted by L, play an important role in (26).

From (26) the behaviour of the flow density in each interface of the membrane can be computed. In particular, for $x = 0$, one concludes that the flow density at feed-membrane interface is given by

$$J_0(t) = -D_{\text{eff}} \frac{\partial u(x,t)}{\partial x}\bigg|_{x=0} = -D_{\text{eff}} \frac{\pi}{2L} \frac{V_{\text{wf}}}{V_0} \sum_{i=1}^{\infty} (2i-1) b_i(t), \tag{27}$$

where $b_i(t)$ are the generalised Fourier coefficients given in (19).

In the same way, if $x = L$ the flow density at the membrane-stripping interface is

$$J_L(t) = -D_{\text{eff}} \frac{\partial u(x,t)}{\partial x}\bigg|_{x=L} = 0,$$

which agrees with the condition (17).

In this interface, $x = L$, a second chemical reaction takes places, where the complex is uncomplexed to form the metal species, who is recovered in the stripping phase. Therefore, the last step of the modelling is to relate the solutions obtained in this section to the velocity equation of the second chemical reaction. A brief description of the modelling in the stripping phase is given in the following section.

2.3. Stripping phase

The aqueous solution present on the opposite side of the membrane, which is initially free from the permeable metal ions, is generally referred to as stripping solution or stripping phase. In the aqueous stripping phase, a stripping agent R is added in order to facilitate the uncomplexation of the metal complex species to the stripping phase. This phase is modelled by a velocity equation relating it with the membrane-stripping interface. The solution of this differential equation simulates the behaviour of the metal species, M_{S}, recovered in the stripping phase. The modelling and the solutions are derived in this section.

The chemical reaction in the membrane-stripping interface is:

$$\overline{C} + R \underset{k'_{\text{r}}}{\overset{k_{\text{f}'}}{\rightleftarrows}} M_{\text{S}} + \overline{E} + X_{\text{S}}, \tag{28}$$

where the metal concentration in the stripping phase, denoted by $[M_{\text{S}}]$, is related to the volume, V_{wS}, and the number of moles, n_{S}, in the stripping phase by $n_{\text{S}} = [M_{\text{S}}]V_{\text{wS}}$. The species responsible for the co-transport is represented for X_{S} in the stripping phase.

The kinetics equations to the reaction (28) are:

$$\begin{aligned} \frac{\mathrm{d}n_S}{\mathrm{d}t} &= k_3 n_{\overline{C}} n_{\text{R}} - k_4 n_{\text{S}} n_{X_{\text{S}}} n_{\overline{E}}, \\ -\frac{\mathrm{d}n_{\overline{C}}}{\mathrm{d}t} &= k_3 n_{\overline{C}} n_{\text{R}} - k_4 n_{\text{S}} n_{X_{\text{S}}} n_{\overline{E}}. \end{aligned} \tag{29}$$

The apparent rate constants deduced from (29) can be expressed as

$$k_3 = \frac{k'_{\mathrm{f}}}{A_{\mathrm{eff}}}, \qquad k_4 = \frac{k'_{\mathrm{r}}}{A^2_{\mathrm{eff}}}. \tag{30}$$

From (29) and taking into account that the number of moles in the membrane-stripping interface is given by $n_{\mathrm{m}}(L,t)$ (see (21)), follows that $\mathrm{d}n_{\overline{C}}/\mathrm{d}t = -\mathrm{d}n_m(L,t)/\mathrm{d}t$, therefore:

$$\begin{aligned} &\frac{\mathrm{d}n_{\mathrm{S}}}{\mathrm{d}t} = \frac{\mathrm{d}n_{\mathrm{m}}(L,t)}{\mathrm{d}t}, \\ &n_{\mathrm{S}}(0) = 0; \quad n_{\mathrm{m}}(L,t) = 0. \end{aligned} \tag{31}$$

The differential equation and initial condition (31) model the growth of the number of moles of the metal in the stripping phase in terms of the number of moles in the membrane-stripping phase interface.

The solution of (31) is found to be

$$n_{\mathrm{S}}(t) = \big(n_0 - n^{\mathrm{f}}_{\infty}\big)\big(1 - \exp(\lambda t)\big) + V_0 \sum_{i=1}^{\infty} (-1)^{i+1} b_i(t), \tag{32}$$

or in terms of the concentration of the metal species in the stripping phase:

$$\big[M_{\mathrm{S}}(t)\big] = \frac{V_{\mathrm{wf}}}{V_{\mathrm{wS}}}(M_0 - M_{\infty})\big(1 - \exp(\lambda t)\big) + \frac{V_{\mathrm{wf}}}{V_{\mathrm{wS}}} \sum_{i=1}^{\infty} (-1)^{i+1} b_i(t). \tag{33}$$

Analysing the solution (32) in the steady state, that is for $t \to \infty$, then one gets that

$$n_{\mathrm{S}}(t) \to n^{\mathrm{S}}_{\infty} = n_0 - n^{\mathrm{f}}_{\infty}. \tag{34}$$

We conclude that in the steady state the number of moles of the species recovered in the stripping phase is given by (34). This means that in the steady state there is no complex in the membrane, and therefore the equilibrium point in terms of concentration in the stripping phases can be to write as

$$M^{\mathrm{S}}_{\infty} = M_0 - M^{\mathrm{f}}_{\infty}. \tag{35}$$

As a final check, note that the number of moles obtained for each the phases satisfies the equality

$$n_{\mathrm{f}}(t) + N_{\mathrm{m}}(t) + n_{\mathrm{S}}(t) = n_0, \quad \forall t \geqslant 0, \tag{36}$$

which is obtained directly from (13), (23) and (32), and which agrees with the mass balance equation for the metal.

In order to test the model it has to be compared with experimental data. Therefore, a simulation by means of a computational algorithm has been developed.

3. Simulation

The process of simulation of the model checked in this work was computed with MATLAB [23]. An algorithm is implemented which includes the initial conditions of the chemical system and the experimental concentration of the metal transported versus time. This algorithm is used to perform a linear interpolation of the difference between the experimental data and the steady state metal concentration in log scale.

The value of the characteristic exponent λ is calculated from the slope of the interpolating polynomial. From this value, the apparent rate velocity k_2 is estimated using the expression (11) for λ. From the value of k_2 and λ, the algorithm of the model presented allows us to simulate the behaviour of the metal concentration in the feed, membrane and stripping phase respectively against time.

The validity of the mathematical model is checked against the experimental data [24] obtained in the transport of hydrochloric acid solution by neutral extractant that corresponds to the system $C^{n+}ML^{n-} + H_mA$ (case 3(a) in table 1).

4. Experimental

4.1. Reagent and solutions

The phospholene used as received, 1-(dodecy-loxy)-3-methyl-1-oxo-Δ^3-phospholene (DMPL), and was kindly donated by Bayer Leverkusen.

A 1 g l^{-1} stock solution of Au(III) containing was prepared from 49% pure solid $HAuCL_4$ (Johnson Mathey) by dilution with HCl. Cumene (A.R. Fluka) was used as diluent.

4.2. Membranes

The flat sheet supported liquid membrane was impregnated with carrier solution containing the extractant dissolved in cumene by immersion for 24 h, then leaving it to drip for a few seconds before being placed in the transport cell.

The flat sheet membrane used was Millipore Durapore GVHP 4700 and the characteristics of the support are summarised in table 2.

Table 2
Initial conditions in the feed phase for the transport of $AuCl_4^-$ in hydrochloric medium.

Metal transported	$AuCl_4^-$
Initial metal concentration	$M_0 = 6.4 \cdot 10^{-5}$ mol/l
Aqueous solution	1 mol/l HCl
Aqueous volume	$V_w = 200$ cm^3
Extraction constant	$K_e = 79.43$ [24]
Stirring speed	1300 rpm

Table 3
Characteristics of the membrane phase for the transport of $AuCl_4^-$ in hydrochloric medium.

Support characteristics	Durapore
	$\varepsilon = 0.75$, $\tau = 1.67$
	$L = 125$ μm, $d = 3.8$ cm
Extractant	$\overline{E}$ = DMPL
Diluent	Cumene

Table 4
Initial conditions in the stripping phase for the transport of $AuCl_4^-$ in hydrochloric medium.

Stripping agent	NaSCN (0.5 mol/l)
PH	2.5
Aqueous volume	$V_w = 200$ cm^3
Stirring speed	1500 rpm

4.3. Transport experiments

The batch transport experiments were carried out in a permeation cell consisting of two compartments made of methacrylate and separated by a microporous membrane. The geometrical membrane area was 15.90 cm^2 and the volume of the feed and stripping solution was 200 ml.

The experiments were performed at 20°C at a mechanical stirring speed of 1300 rpm in the feed and the stripping phase. The experimental and initial conditions of the feed and stripping phase are described in tables 2 and 4.

The aqueous feed solutions contained different concentrations of Au(III) = $AuCl_4^-$ ranging between: $2.5 \cdot 10^{-5}$ mol/l, $6.4 \cdot 10^{-5}$ mol/l, $8.3 \cdot 10^{-5}$ mol/l, $2.4 \cdot 10^{-4}$ mol/l, $4.7 \cdot 10^{-4}$ mol/l.

The permeation of gold was monitored by periodically sampling the feed and stripping phase, and gold was analysed after appropriate dilution by an atomic absorption spectrophotometer Perkin Elmer 2380.

Tables 2–4 shows the initial experimental conditions at 20°C and constant pressure used for the simulation. From the analysis of these initial conditions and the chemical reaction in the feed-membrane interface

$$AuCl_4^- + \overline{E} + H^+ \underset{k_r}{\overset{k_f}{\rightleftarrows}} \overline{HAuCl_4E},$$

it is clear that the transport of Au(III) = $AuCl_4^-$ corresponds to the system $C^{n+}ML^{n-} + H_mA$ with $X_f = H^+$ represented by (5), where $q = 1$ and $[Y] = [A^-] - [C^+]$. Note that $[A^-]$ is the Cl^- concentration and the value of $[C^+]$ is equal to the total metal concentration M_0 (see case 3(a) in table 1).

5. Results and discussion

5.1. *Validity of the mathematical model*

In the present paper, the modelling is applied to the case of an acid solution, and is checked against experimental data corresponding to the transport of $AuCl_4^-$ in hydrochloric acid solution by neutral extractant, and it is shown that the co-transport phenomenon is reproduced with high accuracy.

In figure 3 the experimental data corresponding to the concentration of the $AuCl_4^-$ in the feed phase for different initial metal concentrations [24] are represented up to 90 minutes. In the same figure each solid line is the plot of one solution (13) and it agrees perfectly with the experimental data sets for the first 90 minutes. From this moment on, the solution (13) permits us also to simulate the behaviour of the metal concentration close to steady state.

5.2. *Estimation of the maximal percentage of* Au(III) *transported and the sensitivity of the model with respect to* M_0

The concentration of Au(III) in the steady state given by M_∞ in (10) allows us to estimate theoretically the maximal percentage of transported metal. This percentage has been computed using the relation $M_{\%E} = (M_0 - M_\infty)/M_0 \cdot 100$ and is represented in figure 4 for several initial metal concentrations M_0. In the same figure, it is observed that the maximal percentage of metal transported is constant (88%) for any initial metal concentration M_0 up to $4.7 \cdot 10^{-4}$ mol/l. This behaviour is due to the fact that, in contrast with what happens in the basic medium [13], the acidic medium facilitates the transport of the metal. In spite of the fact that the maximal extraction percentage is constant, the value of the apparent rate constant k_2 (controlling parameter) changes with the different values of the initial concentration M_0. This variation of the controlling parameter k_2 indicates that the speed of the process in the model is sensitive with respect to the initial metal concentration M_0. The caption of figure 3, provides the values of the apparent rate constant k_2 computed by the algorithm using (11).

5.3. *Simulation of the pH in the feed phase*

In the co-transport of the Au(III), the protons are transported with the metal in the stripping phase as shown schematically in figure 2. Therefore, the proton concentration $X_\mathrm{f} = [\mathrm{H}^+]$ in the feed phase decreases during the process as predicted by (5). The equation $\mathrm{pH} = -\log[X_\mathrm{f}]$ permits us to simulate the behaviour of pH in the aqueous feed phase for different experimental data sets as seen in figure 5. From this simulation, it is observed that when the initial metal concentration increases, the model presents variability for the pH. It is important to note that from a mathematical viewpoint, this variability is observed only at 10^{-4} scale for the pH, as is observed in the detailed view in figure 5(b). Therefore, from a chemical viewpoint, this variability can be neglected and it is reasonable to assume that the pH is constant as shown in figure 5(a), for a standard

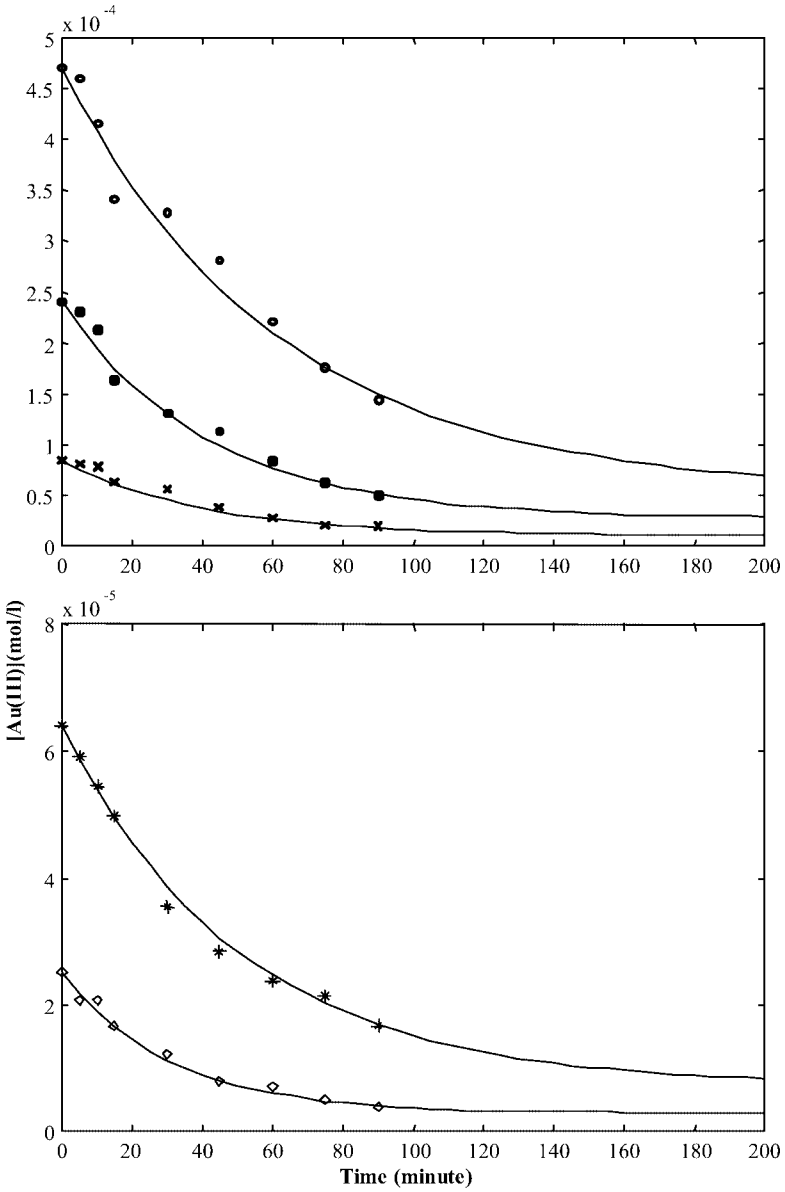

Figure 3. Concentration of $AuCl_4^-$ in the feed phase vs. time for different initial metal concentration M_0 and the same extractant concentration $[\overline{E}] = 0.1$ mol/l. In each checked case, $K_{ex} = 79.43$ and [HCL] = 1 mol/l. □: experimental data for $M_0 = 2.5 \cdot 10^{-5}$ mol/l, $k_2 = 3.6 \cdot 10^{-3}$ min^{-1}. ∗: experimental data for $M_0 = 6.4 \cdot 10^{-5}$ mol/l, $k_2 = 2.2 \cdot 10^{-3}$ min^{-1}. ×: experimental data for $M_0 = 8.3 \cdot 10^{-5}$ mol/l, $k_2 = 2.7 \cdot 10^{-3}$ min^{-1}. ♦: experimental data for $M_0 = 2.4 \cdot 10^{-4}$ mol/l, $k_2 = 2.7 \cdot 10^{-3}$ min^{-1}. •: experimental data for $M_0 = 4.7 \cdot 10^{-4}$ mol/l, $k_2 = 1.8 \cdot 10^{-3}$ min^{-1}. In each case, the solid line is computed from the solution (13) for the feed phase.

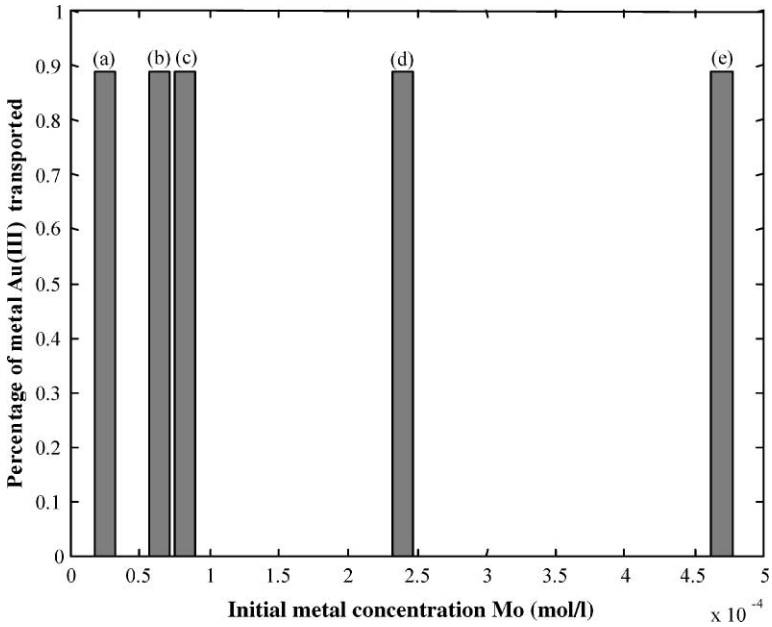

Figure 4. Theoretical maximal percentage $M_{\%E}$ of total metal transported up to steady state M_∞ for different initial metal concentrations M_0 and the same extractant concentration $[\overline{E}] = 0.1$ mol/l and [HCL] = 1 mol/l. (a) $M_0 = 2.5 \cdot 10^{-5}$ mol/l, (b) $M_0 = 6.4 \cdot 10^{-5}$ mol/l, (c) $M_0 = 8.3 \cdot 10^{-5}$ mol/l, (d) $M_0 = 2.4 \cdot 10^{-4}$ mol/l, (e) $M_0 = 4.7 \cdot 10^{-4}$ mol/l.

scale of the pH. Again, this behaviour is different from what happens in the transport of $C^{n+}ML^{n-} + B(OH)_m$ with $X_f = H^+$ (discussed in [13]), which is due to the fact that the equation for the concentration of the species X_f follows a different relation with the metal concentration.

5.4. Sensitivity of the model with respect to the extractant concentration

It is important to note that the model (7) is also sensitive to the extractant concentration $[\overline{E}]$, as shown in figures 6 and 7. This sensitivity can also be explained in terms of the controlling parameter k_2, since $[\overline{E}]$ and k_2 are related by (11).

Figure 6 shows that the solution (13) agrees well with the experimental data corresponding to the transport of Au(III) for different extractant concentration $[\overline{E}]$, while the percentage of metal transported represented in figure 7 has been estimated theoretically by the equation $M_{\%E} = (M_0 - M_\infty)/M_0 \cdot 100$. For instance, when the initial metal concentration is $M_0 = 6.4 \cdot 10^{-5}$ mol/l, it is observed in table 5 that the extraction percentage increases when the extractant concentration does so, in contrast to the constant dependence with respect to the initial metal concentration observed in figure 4. However, a major increase in the extractant concentration does not increase significantly the percentage of metal transported.

To perform the computations of the solution (13) for figures 6 and 7, the charac-

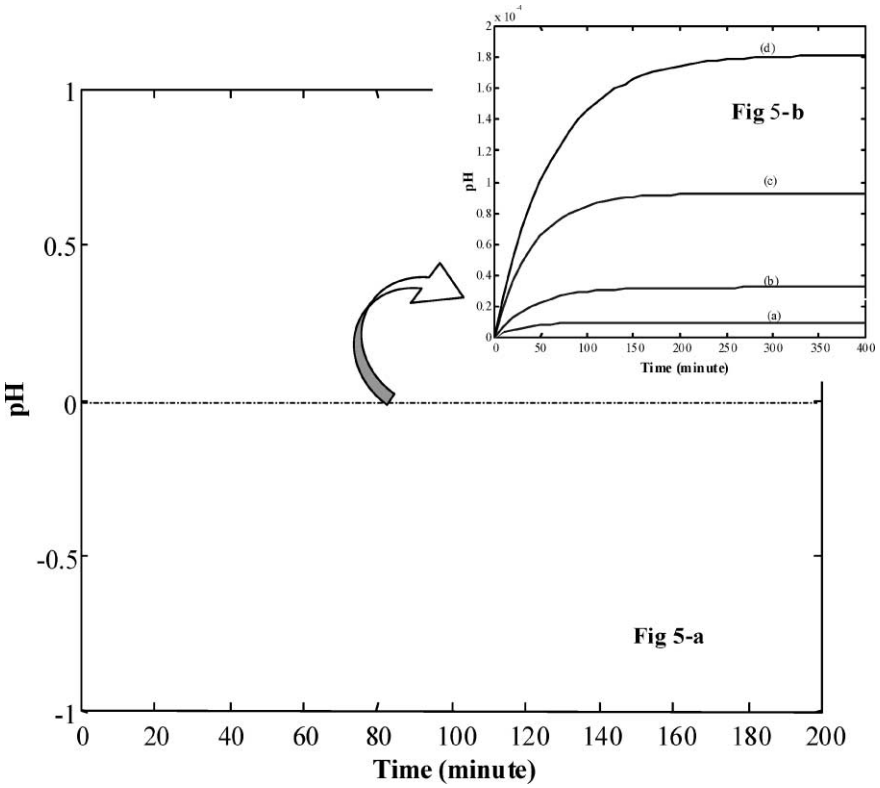

Figure 5. Simulation of the behaviour of the pH in terms of the concentration of the species $X_f = [H^+]$ given by (5). The solid line is the plot of pH vs. time during the transport process up to steady state for different initial metal concentration M_0, $[\overline{E}] = 0.1$ mol/l and [HCL] = 1 mol/l. (a) $M_0 = 6.4 \cdot 10^{-5}$ mol/l, (b) $M_0 = 8.3 \cdot 10^{-5}$ mol/l, (c) $M_0 = 2.4 \cdot 10^{-4}$ mol/l, (d) $M_0 = 4.7 \cdot 10^{-4}$ mol/l.

Table 5
Computed values of the controlling parameter k_2 and extraction percentage $M_{\%E}$ for different extractant concentration and initial metal concentrations $M_0 = 6.4 \cdot 10^{-5}$ mol/l.

$[\overline{E}]$(mol/l), extractant concentration	k_2 ($\min^{-1}$), controlling parameter (apparent rate constant)	$M_{\%E}$, extraction percentage
0.05	$4.9 \cdot 10^{-3}$	79 %
0.1	$2.2 \cdot 10^{-3}$	88 %
0.2	$1.4 \cdot 10^{-3}$	94 %
0.3	$8.9 \cdot 10^{-4}$	96 %

teristic exponent λ was obtained by the algorithm mentioned at the beginning of this section, as the best fitting for each experimental data set, and then k_2 was computed from (11). These values for k_2 and the extraction percentage $M_{\%E}$ are summarised in table 5 for several extractant concentrations.

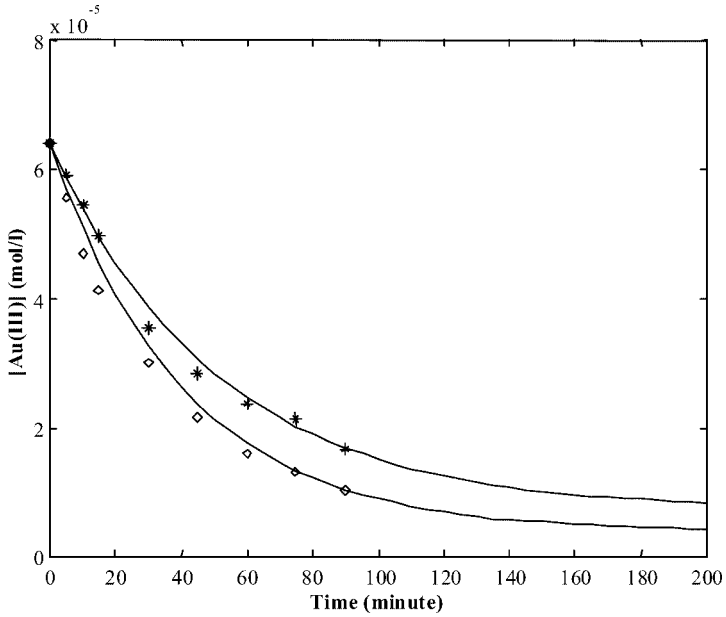

Figure 6. Concentration of Au(III) vs. time in the feed phase for different extractant concentration $[\overline{E}]$, $M_0 = 6.4 \cdot 10^{-5}$ mol/l and [HCL] = 1 mol/l. $*$: experimental data for $[\overline{E}] = 0.1$ mol/l. □: experimental data for $[\overline{E}] = 0.2$ mol/l. The solid line is the plot of the solution (13) in the feed phase.

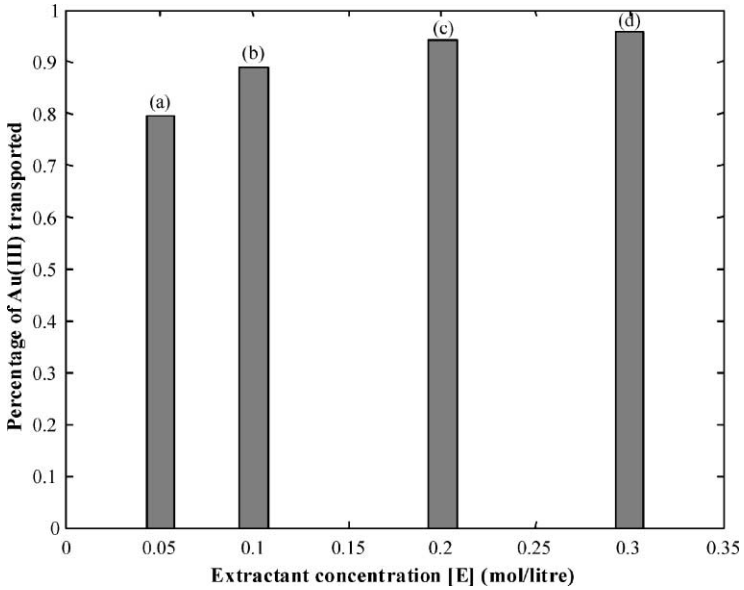

Figure 7. Theoretical extraction percentage $M_{\%E}$ of total metal transported up to steady state for different extractant concentration $[\overline{E}]$ and the same initial metal concentration $M_0 = 6.4 \cdot 10^{-5}$ mol/l. (a) $[\overline{E}] = 0.05$ mol/l, $M_{\%E} = 79\%$, (b) $[\overline{E}] = 0.1$ mol/l, $M_{\%E} = 88\%$, (c) $[\overline{E}] = 0.2$ mol/l, $M_{\%E} = 94\%$, (d) $[\overline{E}] = 0.3$ mol/l, $M_{\%E} = 96\%$.

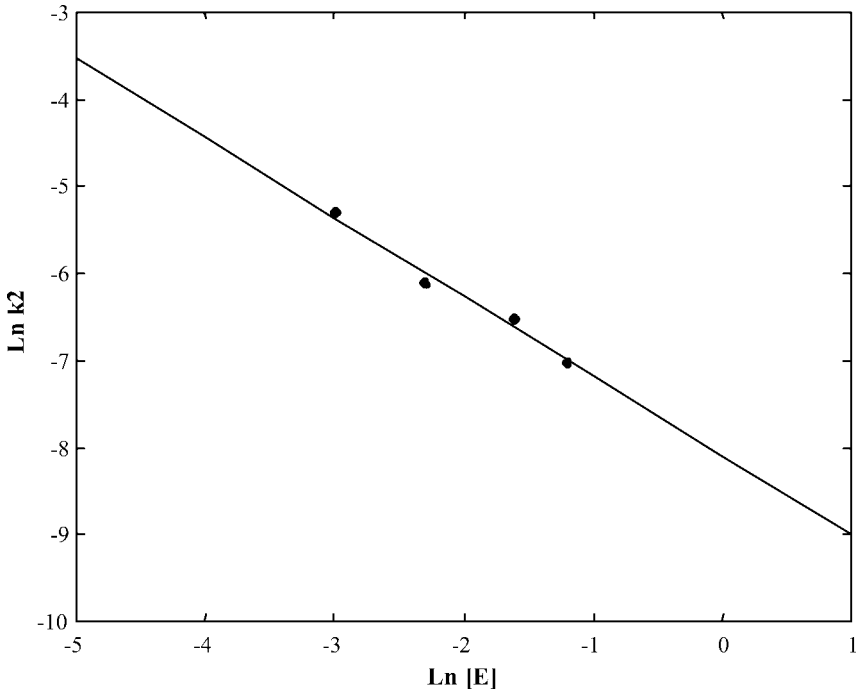

Figure 8. $\ln k_2$ vs. $\ln[\overline{E}]$. •: values obtained from table 5. The straight line is the plot of the linear regression $\ln k_2 = \alpha \ln[\overline{E}] + \ln \beta$, where $\alpha = -0.91$ and $\ln \beta = -8.09$.

In order to obtain the relationship between the controlling parameter k_2, the extractant concentration $[\overline{E}]$ and the initial concentration M_0, we plotted $\ln k_2$ vs. $\ln[\overline{E}]$ and $\ln M_0$, respectively. In the plotting of $\ln k_2$ vs. $\ln M_0$, there is no apparent relation between them, whereas in the plotting of $\ln k_2$ vs. $\ln[\overline{E}]$ (figure 8), a linear regression from the values shown in table 5 allows us to compute $\alpha = -0.91$ and $\beta = 5.1 \cdot 10^{-6}$ in the relation

$$k_2 = \beta\big([\overline{E}]\big)^{\alpha}. \tag{37}$$

It is worth to note that in the system $C^{n+}ML^{n-} + B(OH)_m$ with $X_f = H^+$ developed in [13], the controlling parameter k_2 depends on the initial metal concentration M_0 following the relation $k_2 = \beta([M_0])^{\alpha}$. This different behaviour is to be expected, because the relation (11) for λ in $C^{n+}ML^{n-} + H_m A$ with $X_f = H^+$ (case 3(a) in table 1) is different from the one for λ in the system $C^{n+}ML^{n-} + B(OH)_m$ with $X_f = H^+$. This is due to the different reaction mechanisms of the two systems.

5.5. Simulation of the flow density of the metal-complex trough the membrane

The plot of the flow density and the complex concentration against time are presented in figures 9(a) and 10(a), respectively.

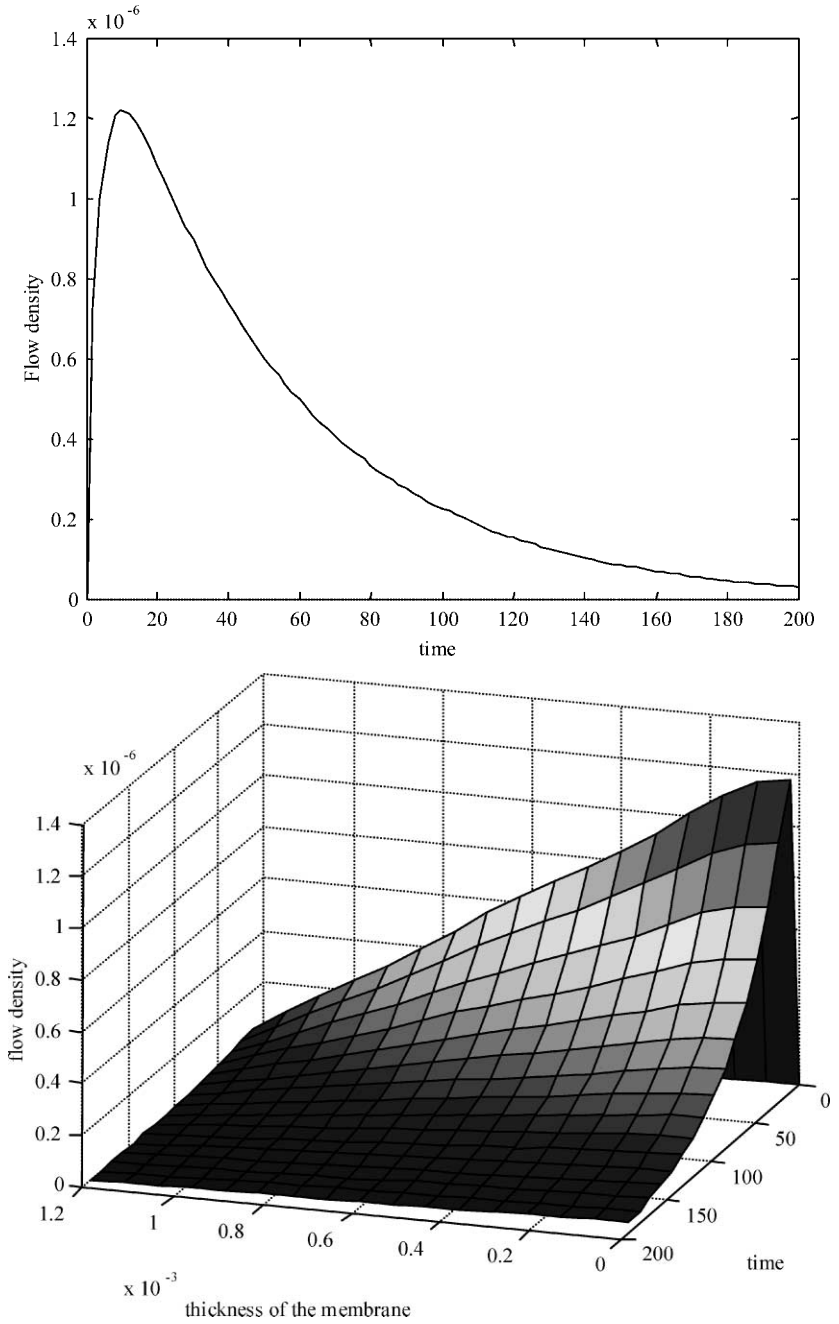

Figure 9. (a) Plot of J_0 vs. t given by (27). Simulation of the flow density of the complex species in the feed-membrane interface. $M_0 = 6.4 \cdot 10^{-5}$ mol/l, $[\overline{E}] = 0.1$ mol/l, [HCL] = 1 mol/l, $k_2 = 2.2 \cdot 10^{-3}$ min^{-1}, $D_{\text{eff}} = 6 \cdot 10^{-7}$ dm^2/min; (b) Plot of J vs. (x, t) given by (26). Simulation of the flow density of the complex species inside the membrane at any time. $M_0 = 6.4 \cdot 10^{-5}$ mol/l, $[\overline{E}] = 0.1$ mol/l, [HCL] = 1 mol/l, $k_2 = 2.2 \cdot 10^{-3}$ min^{-1}, $D_{\text{eff}} = 6 \cdot 10^{-7}$ dm^2/min.

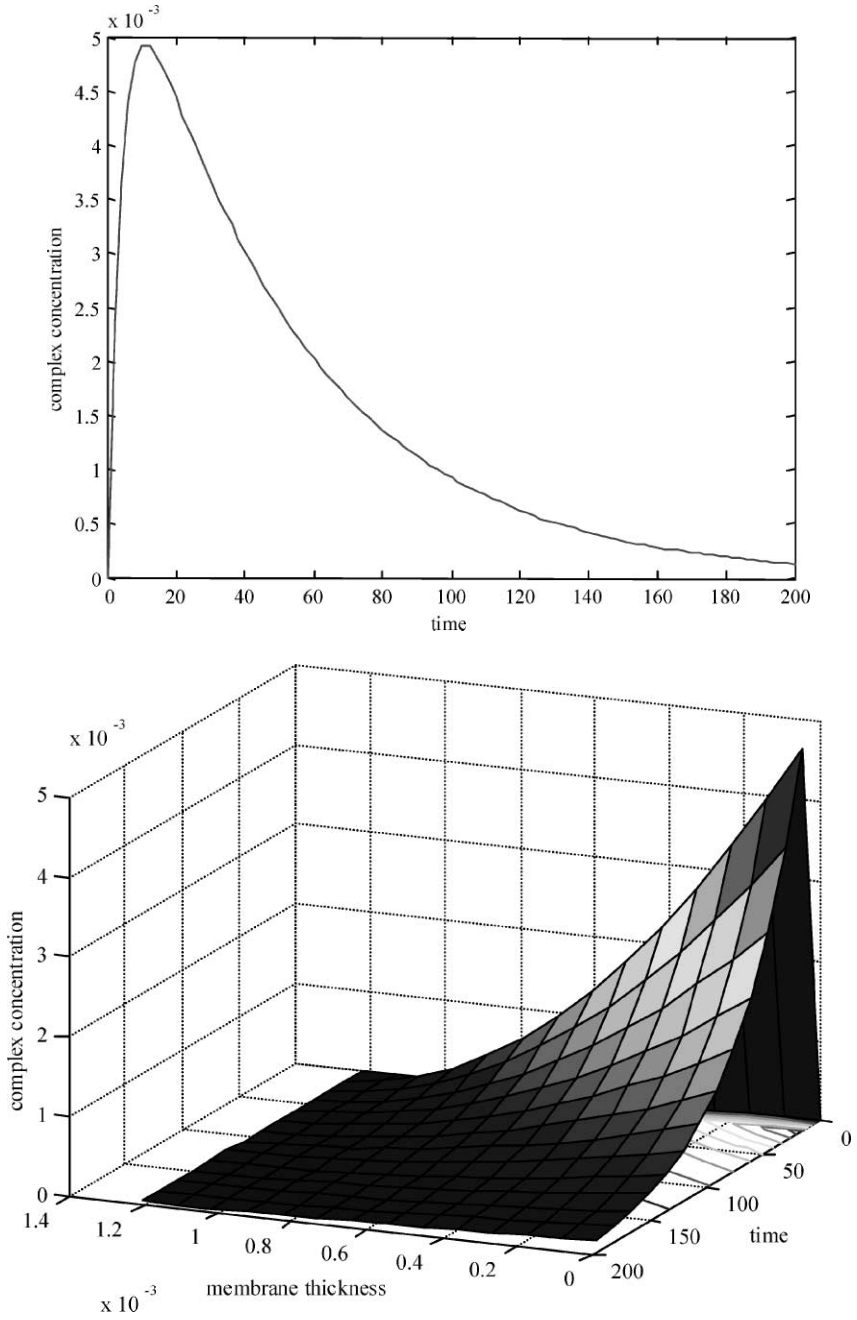

Figure 10. (a) Plot of $\overline{U}$ vs. t (24). Simulation of the behaviour of the complex concentration in the feed-membrane interface ($x = 0$) as a function of time. $M_0 = 6.4 \cdot 10^{-5}$ mol/l, $[\overline{E}] = 0.1$ mol/l, [HCL] = 1 mol/l, $k_2 = 2.2 \cdot 10^{-3}$ min^{-1}, $D_{\text{eff}} = 6 \cdot 10^{-7}$ dm^2/min; (b) Plot of u_m vs. (x, t) given by (25). Simulation of the behaviour of the complex concentration inside the membrane at any time. $M_0 = 6.4 \cdot 10^{-5}$ mol/l, $[\overline{E}] = 0.1$ mol/l, [HCL] = 1 mol/l, $k_2 = 2.2 \cdot 10^{-3}$ min^{-1}, $D_{\text{eff}} = 6 \cdot 10^{-7}$ dm^2/min.

In the three-dimensional figures 9(b) and 10(b) the flow density and complex concentration are plotted as a function of time and of the thickness of the membrane, respectively.

From figures 9(a) and 10(a) one sees that the maximum is attained after a very short time and from that moment on, both the flow density and the concentration of the metal-complex decrease more slowly until almost all of the metal is recovered in the stripping phase.

The dependence on the maximum of the thickness of the membrane can be observed in the three-dimensional figure (figures 9(b) and 10(b)). From these figures one observes the non-linear behaviour of both magnitudes with respect to the thickness.

This non-linearity appears more strongly in the complex concentration plot than in the flow density, $J(x,t)$, which is the derivative of (18) with respect to the thickness.

This behaviour seems to be due to the value of the extractant concentration and the porosity of the membrane.

Numerical simulation of the model, for different values of the thickness of the membrane, shows that this non-linearity is accentuated when the thickness is increased.

5.6. Simulation of the behaviour of the metal in the membrane phase and the stripping phase

Figure 11(a) provides a plot of the metal concentration in the three phases. The experimental data corresponds to the feed phase. Since there are no experimental data for the stripping and membrane phases, only the simulation produced by the model is plotted.

In figure 11(b), a simulation of the number of moles in each phase given by the solution (12), (23) and (32) has been plotted, together with equation (36) as a final check. One sees from figure 11(b) that the mass balance equation given by equation (36) is satisfied.

6. Conclusions

A mathematical model is derived that describes the transport of metal species through a flat sheet support liquid membrane (FSSLM) in transition state is derived. From this model, the diffusion inside the membrane phase is modelled by Fick's second law and the flow density of the metal complex species is modelled by Fick's first law.

One of the features of the model is that it takes into account the chemical reaction at the interface and the driving force between the feed and stripping phase. This allows us to reproduce and simulate the evolution of the metal species in each phase, together with the evolution of the pH in the feed phase in transition state.

The value of the rate constant, which is the controlling parameter of the speed of the process, is estimated from the kinetics of the chemical reaction.

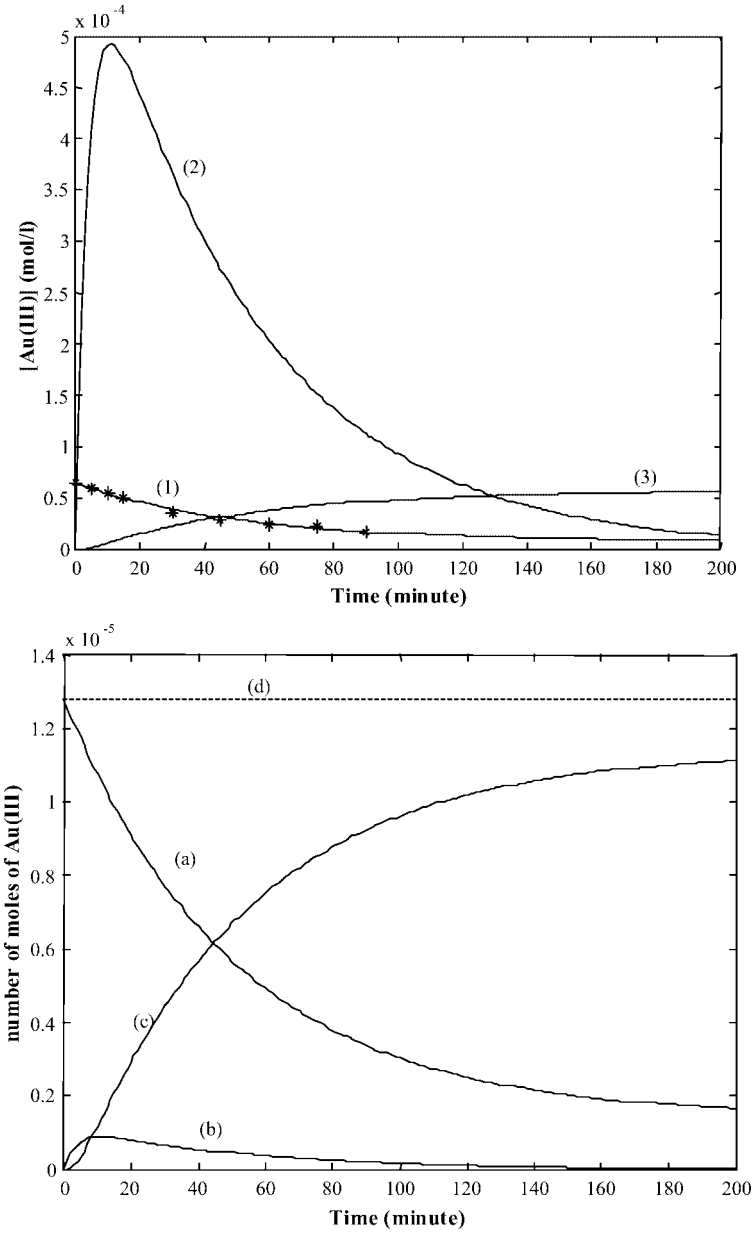

Figure 11. (a) Simulation of the behaviour of the metal species Au(III) in the three phases. $M_0 = 6.4 \cdot 10^{-5}$ mol/l, $[\overline{E}] = 0.1$ mol/l, [HCL] = 1 mol/l, $k_2 = 2.2 \cdot 10^{-3}$ min^{-1}. $D_{\text{eff}} = 6 \cdot 10^{-7}$ dm^2/min. (1) $*$: experimental data for feed phase. The solid line is the plot of solution (13) for $[M_{\text{f}}]$ vs. time. (2) $\overline{U}$ vs. time. The plot of the solution (24) for membrane phase. (3) $[M_{\text{S}}]$ vs. time. The plot of the solution (33) for stripping phase; (b) Evolution of the number of moles of the metal species Au(III) in the different phases: (a) $n_{\text{f}}(t)$ number of moles in the feed phase, (b) $0.1 \cdot n_{\text{m}}(t)$ number of moles in the membrane phase (0.1 is a scale factor for a better visualisation), (c) $n_{\text{S}}(t)$ number of moles in the stripping phase, (d) Plot of the mass balance equation $n_{\text{f}} + n_{\text{m}} + n_{\text{S}}$.

The model reproduces with high accuracy the transport of metal ions in acidic solution when checked against experimental data corresponding to the transport of $AuCl_2^-$ in hydrochloric acid solution.

7. Nomenclature

A_{eff}	effective interfacial area (dm^2);
$b_i(t)$	temporal Fourier coefficients;
C	metal ion species in the membrane and stripping phase;
$[C]$	metal ion concentration in the membrane and stripping phase (mol/l);
d	membrane diameter (dm);
D_{eff}	effective membrane diffusion coefficient of the metal in the organic phase (dm^2/min);
D_E	diffusion coefficient of the extractant in the membrane phase (dm^2/min);
$\overline{E}$	extractant (carrier) species in the membrane phase;
$[\overline{E}]$	extractant concentration (mol/l);
$J(x, t)$	flow density of the complex in terms of time and the thickness of the membrane mol/(min dm^2);
$J(t)$	flow density of the complex in feed-membrane interfaces (mol/(min dm^2));
k_{f}	forward rate constant of the chemical reaction in the feed-membrane interface ((dm^2)^2/(mol^2 min));
k'_{f}	forward rate constant of the chemical reaction in the membrane-stripping interface;
k_{r}	reverse rate constant of the chemical reaction in the feed-membrane interface (min^{-1});
k'_{r}	reverse rate constant of the chemical reaction in the membrane-stripping interface;
k_1	apparent forward rate constant (1/mol^2 min);
k_2	apparent reverse rate constant. Controlling parameter (min^{-1});
K_{ex}	extraction constant at feed-membrane interface;
K_{W}	ionic product of water;
K	proportionality constant;
L	membrane thickness (cm);
M_{f}	metal species in the feed phase;
M_0	initial metal concentration in the feed phase (mol/l);
$M_{\%E}$	metal extraction percentage;
M_∞	equilibrium point. Value of the metal concentration in the aqueous feed phase when the steady state is achieved (mol/l);
$[M_{\text{f}}]$	metal concentration in the feed phase as a function of time (mol/l);
$[M_{\text{S}}]$	metal concentration in the stripping phase as a function of time (mol/l);
n^{S}_∞	equilibrium point. Value of the number of moles of the metal species in the stripping phase at any time (mol);
m, n	represent the charge of ions (see table 1);

n_0 initial number of moles of the metal species in the feed phase (mol);
n_∞^{f} number of moles in the feed phase in the steady state (mol);
$n_{\mathrm{f}}(t)$ number of moles in the feed phase at time t (mol);
$n_{\mathrm{m}}(0,t)$ number of moles in the feed-membrane interface at time t (mol);
$n_{\mathrm{m}}(L,t)$ number of moles in the second interface at time t (mol);
$n_{\mathrm{m}}(t)$ number of moles in the membrane phase at time t (mol);
$n_{\mathrm{S}}(t)$ number of moles in the stripping phase at time t (mol);
R stripping reagent (mol/l);
$\Re$ real field;
t time variable (min);
$u(x,t)$ complex concentration in membrane phase as a function of time and the thickness of the membrane (mol/l);
$u(0,t)$ complex concentration at feed-membrane interface (mol/l);
$u(L,t)$ complex concentration at membrane-stripping interface (mol/l);
$\overline{U}(t)$ concentration of the complex in the membrane phase (mol/l);
V_0 organic volume (dm^3);
V_{wf} aqueous volume in the feed phase (dm^3);
V_{wS} aqueous volume in the stripping phase (dm^3);
X_{f} species whose gradient between the feed and stripping phase is the driving force of the process;
$[X_{\mathrm{f}}]$ concentration of the species X_{f} as a function of time (mol/l);
x space variable (dm).

Greek letters

ε porosity of the SLM;
τ tortuosity of the membrane;
α linear coefficient in the linear regression;
β independent coefficient in the linear regression;
λ eigenvalue obtained of the stability study (min^{-1});
λ_i eigenvalues obtained using separation of variables and Fourier series;
$\phi_i(x,\lambda_i)$ eigenfunctions corresponding to λ_i;
π pi number.

Subscripts

f and S refers to feed and stripping solutions, respectively;
w refers to the aqueous phase;
o refers to the organic phase;
∞ infinity time or steady state.

Acknowledgements

This work was supported by the MCYT (PPQ2002-04267) and DURSI SGR2001-00249. G. Benzal gratefully acknowledges economic support from FOMEC for the fellowship at the Universidad Nacional de Tucumán, Tucumán, Argentina.

References

[1] R.A. Bartsch and J.D. Way, In chemical separations with liquid membranes, in: ACS Sympos. Ser., No. 642 (American Chemical Society, Washington, DC, 1996) chapter 1, pp. 1–10.

[2] A.M. Sastre, A. Kumar, J.P. Shukla and R.K Singh, Improved technique in liquid membrane separation: A review, Separation and Purification Methods 27 (1998) 213–298.

[3] W.S.W. Ho and K.K. Sirkar, *Membrane Handbook* (Van Nostrand-Reinhold, New York, 1992).

[4] J. de Gyves and E. Rodrigues de San Miguel, Metal ion separations by supported liquid membranes, Ind. Eng. Chem. Res. 38(6) (1999) 2182–2202.

[5] L.A.J. Chrisstoffels, F. de Jong and D. Reinhoudt, in: ACS Sympos. Ser., No. 642 (American Chemical Society, Washington, DC, 1996) chapter 3, p. 18.

[6] R.T. Peterson and J. Lamb, in: ACS Sympos. Ser., No. 642 (American Chemical Society, Washington, DC, 1996) chapter 4, p. 57.

[7] B.M. Misra, J.S. Gill, in: ACS Sympos. Ser., No. 642 (American Chemical Society, Washington, DC, 1996) chapter 25, p. 361.

[8] P.R. Danesi, E.P. Horwitz, G.F. Vandegrift and R. Chiarizia, Mass transfer rate through liquid membrane: Interfacial chemical reactions and diffusion as simultaneous permeability controlling factors, Sep. Sci. Technol. 16(2) (1981) 201.

[9] I. Komasawa, T. Otake and T. Yamashita, Mechanism and kinetics of copper permeation through a supported liquid membrane containing a hydroxyoxime as a mobile carrier, Indian Eng. Chem. Fundament. 22 (1983) 127.

[10] P. Plucinski and W. Nitsch, The calculation of permeation rates through supported liquid membranes based on the kinetics of liquid-liquid extraction, J. Membr. Sci. 39 (1988) 43.

[11] R.B. Bird, W.E. Stewart and E.N. Lightfoot, *Fenómenos de transporte* (Reverté, 1992).

[12] P.R. Danesi, Solvent extraction kinetics, in: *Principles and Practice of Solvent Extraction*, eds. J. Rydberg, C. Musikas and G.R. Chopin (Marcel Dekker, New York, 1992).

[13] G. Benzal, A. Kumar, A. Delsham and A.M. Sastre, Mathematical modelling of co-transport phenomena through a flat sheet supported liquid membrane. Simulation of the transport of metal anions in alkaline solution, Hydrometallurgy (2003), in press.

[14] M.W. Hirsch and S. Smale, *Differential Equations, Dynamical Systems and Linear Algebra* (Alianza Editorial, Madrid, 1983).

[15] J. Palis Jr. and W. de Melo, *Geometric Theory of Dynamical Systems* (1998).

[16] E.L. Cussler, *Diffusion. Mass Transfer in Fluid Systems* (Cambridge University Press, 1997).

[17] J. Bear, *Dynamics of Fluid in Porous Media* (Dover Publications, 1972).

[18] J. Crank, *The Mathematics of Diffusion* (Oxford Science Publications, 1975).

[19] R. Haberman, *Elementary Applied Partial Differential Equations*, 3rd ed. (Prentice Hall, New York, 1998).

[20] E.C. Zachmanoglou and D.W. Thoe, *Introduction to Partial Differential Equations with Applications* (Dover, New York, 1986).

[21] T.-C. Huang and R.-S. Juang, Rate and mechanism of divalent metal transport through supported liquid membrane containing Di(2-ethylhexyl) phosphoric acid as a mobile carrier, J. Chem. Tech. Biotechnol. 42 (1988) 3–17.

[22] J.A. Ibáñez, L. Victoria and A. Hernández, Flow and characteristic parameters in mediated transport through liquid membranes, A theoretical model, Sep. Sci. Technol. 24(1,2) (1989) 157.

[23] MATLAB, The Language of Technical Computing, Version 6.0, Release 12 (The MathWorks, 2000).

[24] A. Madi, Doctoral Thesis, Universitat Politècnica de Catalunya, Spain (1998).